

## Invariants and Geometric Structures in Nonlinear Hamiltonian Magnetic Reconnection

E. Cafaro,<sup>1</sup> D. Grasso,<sup>1,2</sup> F. Pegoraro,<sup>2,3</sup> F. Porcelli,<sup>1</sup> and A. Saluzzi<sup>1,4</sup>

<sup>1</sup>*Energetics Department, Politecnico di Torino, INFN Torino, Italy*

<sup>2</sup>*Physics Department, University of Torino, INFN Torino, Italy*

<sup>3</sup>*Physics Department, University of Pisa, INFN Pisa, Italy*

<sup>4</sup>*Alenia Spazio SpA, Torino, Italy*

(Received 22 August 1997)

Collisionless magnetic reconnection in a two dimensional plasma is analyzed, using a two-fluid model where electron mass and pressure effects are important. Numerical simulations show the formation of current and vorticity layers along two branches crossing at the stagnation point of the plasma flow. These structures are interpreted on the basis of the Hamiltonian Casimirs (conserved fields) of the fluid plasma model. [S0031-9007(98)06155-9]

PACS numbers: 52.35.Py, 47.65.+a, 52.65.Kj, 94.30.Gm

The problem of magnetic reconnection in collisionless regimes was originally motivated by applications to space plasma processes, such as reconnection events occurring in the Earth magnetotail [1]. Renewed interest in this problem was prompted by the observation of fast relaxations in high temperature laboratory plasmas of thermonuclear interest. One well known example is the so called "sawtooth crash" of the central temperature of a tokamak plasma, which may occur on a time scale short compared to the average electron-ion collision time [2]. Recently it was shown [3,4] that electron inertia may account for the fast time scales observed in the experiments.

The first aim of this Letter is to extend this analysis to finite temperature regimes, where electron pressure effects are important. We find that in the early nonlinear phase the growth of the magnetic island is even faster than in the cold electron limit of Ref. [4]. The fast collisionless evolution in this early nonlinear regime is a non-steady-state process, characterized by the formation of increasingly narrower microscales below the electron skin depth. The long term behavior is likely to require kinetic considerations outside the scope of the fluid model adopted in this paper.

The second aim is the investigation of the role played by the Casimir invariants. Indeed, it can be shown that the adopted collisionless model admits a Hamiltonian structure [5,6]. While magnetic flux is reconnected in the course of plasma evolution, the conserved fields associated with the Casimirs preserve their initial topology. The nature of collisionless reconnection under these circumstances is entirely different from that of resistive reconnection.

The model we consider is an extension of reduced magnetohydrodynamic [7] to a two-fluid description, where electron inertia, associated with the inertial skin depth,  $d_e = c/\omega_{pe}$ , and the electron pressure terms are retained in the generalized Ohm's law [8] (a more general model is the four field model of Ref. [9]). More specifically, we adopt an isothermal equation of state for the electrons and disregard diamagnetic effects associated

with equilibrium pressure gradients, a valid approximation as long as the electron diamagnetic frequency is small compared with the characteristic growth rate of the reconnection process. On the other hand, we retain the divergence of the electron stress tensor (electron gyroviscosity) in the generalized Ohm's law. The parallel electron compressibility introduces the characteristic scale length,  $\varrho_s = \sqrt{T_e/m_i}/\omega_{ci}$ , related to the ion inertia and to the electron temperature,  $T_e$ . The cold electron regime is defined by the limit  $\varrho_s/d_e \rightarrow 0$ . We also consider the limit where the ion Larmor radius,  $\varrho_i = \sqrt{T_i/m_i}/\omega_{ci}$ , is neglected. In linear theory,  $\varrho_i$  enters on equal footing with  $\varrho_s$  in determining the growth rate [10,11]. In addition, the Hamiltonian structure is preserved even with  $\varrho_i$  terms retained [6]. Thus we may expect that  $\varrho_i$  terms will not change the qualitative behavior obtained here below in the limit  $\varrho_i \rightarrow 0$ .

The 2D model equations we consider are [8]

$$\frac{dF}{dt} = \varrho_s^2 [U, \psi], \quad (1)$$

$$\frac{dU}{dt} = [J, \psi]. \quad (2)$$

Here the time is normalized on the Alfvén time,  $\tau_A$ ,  $d_e \equiv d_e/L_x$  and  $\varrho_s \equiv \varrho_s/L_x$ , where  $L_x$  is the characteristic macroscopic length. The magnetic field is  $\mathbf{B} = B_0 \mathbf{e}_z + \nabla \psi \times \mathbf{e}_z$ , with  $B_0$  constant and  $z$  the ignorable coordinate. The  $\mathbf{E} \times \mathbf{B}$  drift on the normal plane is  $\mathbf{v}_\perp = \mathbf{e}_z \times \nabla \varphi$ , where  $\varphi$  is a stream function,  $U = \nabla^2 \varphi$  is the corresponding vorticity,  $J = -\nabla^2 \psi$  is the current density, and  $F = \psi + d_e^2 J$  is the  $z$  component of the velocity-space averaged canonical momentum. The Poisson brackets are defined as  $[A, B] = \mathbf{e}_z \cdot \nabla A \times \nabla B$  and the total time derivative is defined as  $d/dt \equiv \partial/\partial t + [\varphi, \ ]$ . The first equation corresponds to Ohm's law in which electron inertia, the electron pressure gradient, and the electron stress tensor are considered. The second equation is the vorticity equation.

These equations can be written in the following conservative form:

$$\frac{d_{\pm}G_{\pm}}{dt} = 0, \quad (3)$$

where we have defined the fields

$$G_{\pm} \equiv F \pm d_e \varrho_s U. \quad (4)$$

The total time derivative is  $d_{\pm}/dt \equiv \partial/\partial t + [\varphi_{\pm}, ]$  where the generalized stream functions are defined as [6]:  $\varphi_{\pm} \equiv \varphi \pm (\varrho_s/d_e)\psi$ . Since the fields  $G_{\pm}$  are conserved as they are advected by the generalized velocities  $\mathbf{v}_{\pm} = \mathbf{e}_z \times \nabla \varphi_{\pm}$ , their topology remains frozen during the time evolution of the system ( $\mathbf{v}_{\pm}$  are smooth functions of  $x$ ,  $y$ , and  $t$ ).

The mathematical model can also be cast in noncanonical Hamiltonian form with the Hamiltonian functional given by (modulo addition of Casimirs [6]):

$$H = \frac{1}{2} \int d^2x (|\nabla \psi|^2 + d_e^2 J^2 + \varrho_s^2 U^2 + |\nabla \varphi|^2). \quad (5)$$

Two infinite sets of Casimirs can also be defined:

$$C_{\pm} = \int d^2x h_{\pm}(G_{\pm}) \quad (6)$$

with  $h_{\pm}$  arbitrary functions. The Casimirs are constants of motion of our system of equations. In the limit of vanishing  $\varrho_s$ , upon expanding  $h_{\pm}$  to first order, we find the Casimirs of the cold electron case,  $C_1 = \int d^2x h_1(F)$  and  $C_2 = \int d^2x U h_2(F)$ . In this case, the canonical momentum  $F$  is conserved and its topological structure is preserved in time. We point out that the topological transition of  $F$  requires both finite  $\varrho_s$  and finite electron inertia. This can be seen by rewriting Eq. (1) as

$$\frac{\partial F}{\partial t} + [\varphi - \varrho_s^2 U, F] = d_e^2 \varrho_s^2 [J, U]. \quad (7)$$

Thus, for  $d_e \varrho_s \rightarrow 0$ ,  $F$  is written in Lagrangian conservative form. The last term in Eq. (7), which is responsible for the topological transition of  $F$ , is related to the off-diagonal terms of the electron stress tensor. It expresses the fact that the magnetic flux  $\psi$  and the current density  $J$  are advected with different velocities: the first with the particle and the second with the gyrocenter fluid velocity.

We consider the large  $\Delta'$  regime, defined by  $\Delta' d_e > (d_e/\varrho_s)^{1/3}$ , which allows [4,12] an early nonlinear phase during which fast magnetic reconnection can take place. The linear system obtained from Eqs. (1) and (2) was solved analytically in Ref. [11]. In the relevant limit  $\varrho_s > d_e$ , the linear growth rate normalized to the Alfvén time is  $\gamma_L \sim (2d_e \varrho_s^2/\pi)^{1/3}$  (the parameter  $\Delta'$  measures the logarithmic jump of  $\psi$  across the reconnection layer [13]). In this linear regime, the mode structure exhibits macroscopic convection cells, with characteristic size  $L_{\text{cell}} \sim L_x$ , the vorticity profile has a width  $\sim \varrho_s$ , while the current density has a width of  $\sim d_e$ , with a tail extending over a distance  $\sim \varrho_s$ . Note that, already in linear

theory, one can see an enhancement of the reconnection rate, by a factor  $(\varrho_s/d_e)^{2/3}$  compared with the growth rate obtained for  $\varrho_s < d_e$ .

In this paper, we present the numerical solution of the nonlinear Eqs. (1) and (2) obtained by means of the finite difference method on a nonuniform grid. The numerical integration strategy is such that the discretization error for the space operators can be assumed asymptotically of second order. We assume a two dimensional slab with aspect ratio  $\epsilon = L_x/L_y$  and double periodic boundary conditions, equilibrium fields  $\psi_{\text{eq}} = \cos x$ ,  $\varphi_{\text{eq}} = 0$ , and initial perturbations  $(\varphi, \delta\psi) = \text{Re}\{[\varphi(x), \delta\psi(x)]e^{\gamma t + iky}\}$ . Our results for the case  $\varrho_s \rightarrow 0$  were first reported in Ref. [14]. These results confirm the formation of a current layer along the neutral line with a sublayer characterized by a microscale, which shrinks with time as  $\delta(t) \sim d_e \exp[-w(t)/2d_e]$ , where  $w$  is the magnetic island width, in agreement with the analysis of Ref. [4].

New numerical solutions obtained for parameter values  $\varrho_s = 3d_e$  and  $\varrho_s = d_e/2$ , at fixed aspect ratio  $\epsilon = 1/2$  and inertial skin depth  $d_e = 0.08$  are shown in Figs. 1 and 2. In particular, Fig. 1 shows the contour plots of the fields  $\psi$ ,  $\varphi$ ,  $J$ ,  $U$ ,  $F$ ,  $G_+$ , and  $\varphi_+$  for the case  $\varrho_s = 3d_e$  at a time such that the ratio of the magnetic island width over the inertial skin depth is  $\approx 3.5$ . (Note that the contour lines of  $G_+$  are very close to those of  $\psi$  for this case, where  $\varrho_s > d_e$ .) Figure 2 shows the profiles of the quantities  $\delta\psi = \psi - \psi_{\text{eq}}$ ,  $\varphi$ ,  $J$ , and  $G_+$  across the neutral line at different simulation times for  $\varrho_s = d_e/2$ . From Figs. 2(a) and 2(b) we see that  $\delta\psi$  and the stream function  $\varphi$  vary over a region of order  $\varrho_s \sim d_e$ . On the contrary, the profiles of the current density  $J$  and of the conserved field  $G_+$  develop a narrow sublayer below the skin depth, similarly to the case  $\varrho_s = 0$ .

The amount of reconnected flux, as measured by  $\delta\psi_X \equiv \psi(0, 0; t) - \psi_{\text{eq}}(0)$  (the magnetic flux function at the  $X$  point,  $x = y = 0$ ), scales as  $\delta\psi_X \sim -w^2(t)/8$ , as can be shown by simple analytic considerations. The island width grows to macroscopic values in the early nonlinear phase, i.e.,  $L_{\text{cell}} > w(t) \geq d_e, \varrho_s$ ; hence the amount of reconnected flux tends to become of order unity. Likewise, the peak value of the current density increases with the square of the magnetic island width. Note that  $U$  is an odd function of  $x$  and  $y$  and the origin is a stagnation point of the flow. Hence,  $(\delta G_+)_X = \delta\psi_X + d_e^2 \delta J_X = 0$ , from which  $\delta J_X \sim w^2(t)/8d_e^2$ . Clearly, this result is strictly valid in the absence of dissipation.

Figure 1(h) illustrates the time evolution of  $\ln[w(t)/d_e]$ . This figure compares the cases  $\varrho_s = d_e/2$  and  $\varrho_s = 3d_e$ . In both cases, the growth of  $w(t)$  is faster than exponential and indicative of a quasiexplosive behavior in the early nonlinear phase, as discussed in [4] for the case  $\varrho_s = 0$ . The growth rate is larger at larger values of  $\varrho_s/d_e$ . Although the precise scaling law is difficult to obtain numerically, these results suggest that the magnetic island attains a macroscopic amplitude on the time scale  $\tau \sim \gamma_L^{-1} \sim \varrho_s^{-2/3} d_e^{-1/3} (\varrho_s > d_e)$ .

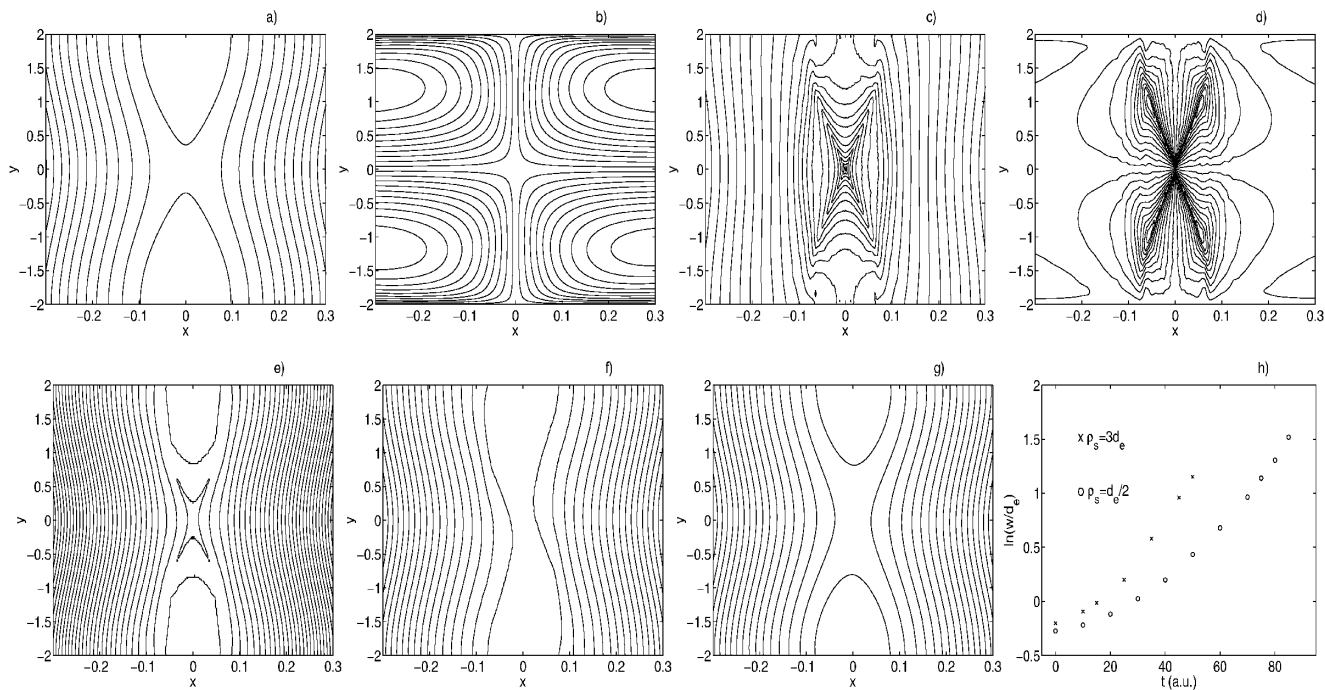


FIG. 1. Contour plots for the case  $\varrho_s = 3d_e$ ,  $d_e = 0.08$ , and  $\epsilon = 1/2$  at a time such that  $w(t)/d_e \approx 3.5$ : (a)  $\psi$ ; (b)  $\varphi$ ; (c)  $J$ ; (d)  $U$ ; (e)  $F$ ; (f)  $G_+$ ; (g)  $\varphi_+$ . (h)  $\ln(w(t)/d_e)$  for different values of  $\varrho_s$ . The  $x$  and  $y$  coordinates are normalized on the scale length  $L_x$ .

In the finite  $\varrho_s$  regime, in contrast with the limit  $\varrho_s \rightarrow 0$ ,  $F$  changes its topology: one  $O$  point forms at the origin and four stationary points form symmetrically around it, as shown in Fig. 1(e). The initial topology of the  $G_{\pm}$

fields is preserved, as shown in Fig. 1(f). Figure 2(g) shows the contour lines of  $\varphi_+$ . The contour levels of  $G_-$  and  $\varphi_-$  are symmetric to those of  $G_+$  and  $\varphi_+$ .

A cross-shaped configuration in the current density and vorticity layers is shown in Figs. 1(c) and 1(d). The current density layer is split into two branches, while two layers of vorticity with opposite signs are formed along these branches. This is a distinctly new feature as compared with the cold electron case. The formation of the cross shape can be interpreted in terms of the time evolution of the conserved fields,  $G_{\pm}$ . Initially, these two fields have vertical contour lines, with a neutral line (i.e., a line where  $\nabla G_{\pm} = 0$ ) along the  $y$  axis. As the instability evolves, the contour lines of  $G_+$  and  $G_-$  rotate in opposite directions: the neutral lines do not coincide any longer and, if superimposed, form a cross. The rotation is introduced by the velocity fields  $\mathbf{v}_{\pm} = \mathbf{e}_z \times \nabla \varphi_{\pm}$ . Since  $G_{\pm}$  are advected by  $\mathbf{v}_{\pm}$ , the neutral lines of  $G_{\pm}$  (on which  $\partial G_{\pm} / \partial t = 0$ ) at a nonlinear time (such that  $w > d_e$ ) tend to align along the branches of the separatrices of  $\varphi_{\pm}$ . Using the ansatz near the origin suggested by the numerical simulation (see also Ref. [4]),  $\varphi \sim \varphi_0(t) (x/\delta) \sin(y)$ ,  $\psi \sim \cos(x) + \psi_0(t) \cos(y)$ , with  $\varphi_0 \sim -\lambda \sim -\gamma\lambda$ ,  $\lambda \sim w/2$  is the fluid displacement along  $x$  for  $|x| > \delta \sim \gamma$  and  $\psi_0 \sim -\lambda^2/2$ , we can readily estimate the angle  $\theta$  between the  $x$  axis and the direction of  $\mathbf{v}_+$ . For  $\varrho_s/d_e \rightarrow 0$ , this angle is either 0 or  $\pi/2$ , i.e.,  $\mathbf{v}_+$  is aligned along either the  $x$  axis or the  $y$  axis and no rotation is induced. For  $\varrho_s/d_e > 1$ , we find instead

$$\tan \theta \sim \pm \sqrt{|\psi_0|} \sim \pm w/2\sqrt{2}. \quad (8)$$

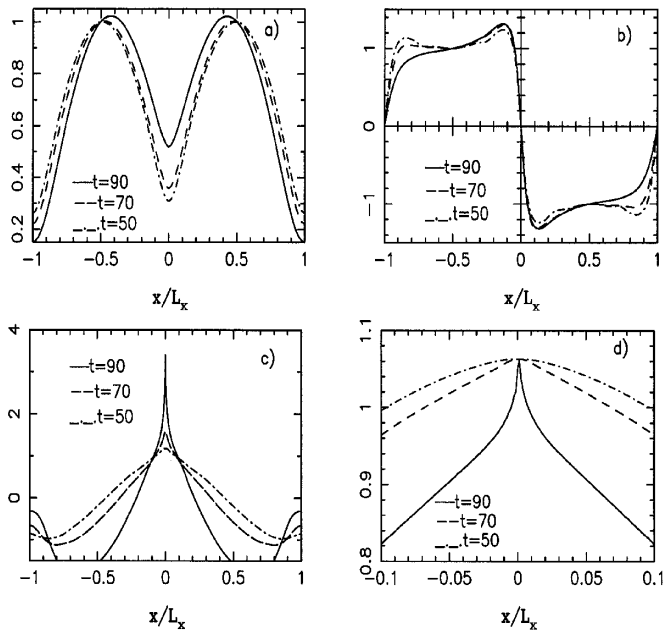


FIG. 2. Cross sections at constant  $y$  for the case  $\varrho_s = d_e/2$ : (a)  $\delta\psi/(\delta\psi)_{x=L_x/2}$  at  $y=0$ ; (b)  $\varphi/(\varphi)_{x=-L_x/2}$  at  $y=L_y/4$ ; (c)  $J$  at  $y=0$ ; (d)  $G_+$  at  $y=0$ .  $t=50$  corresponds to  $w/d_e \approx 1.7$ ,  $t=70$  to  $w/d_e \approx 2.7$ , and  $t=90$  to  $w/d_e \approx 5.6$ .

In this case the asymptotes of the hyperbolic stream functions  $\varphi_{\pm}$  tend to be tangent to the separatrix of  $\psi$  at the origin. Since  $w(t)$  tends to grow to macroscopic values, there is no indication of saturation of the angle  $\theta(t)$  in the early nonlinear stage when  $\varrho_s > d_e$ .

As a test of the validity of our results, we have checked the relative changes of the energy  $H$  and of the invariant  $g_+ \equiv \int G_+ d^2x$ . Clearly, the exact solution of Eqs. (1) and (2) should conserve  $H$  and  $g_+$  exactly. We find that  $H$  varies less than 1% and  $g_+$  less than 4% at the end of the integration period. The numerical inaccuracy in the conservation of  $H$  and  $g_+$  is related to the microscale, which becomes narrower in time. Our simulations stop at a time when the microscale has become so narrow that it can no longer be satisfactorily resolved by our numerical grid. Up to this time, there is no indication of saturation of  $w(t)$ . With the introduction of a viscosity operator, we have been able to reach larger values of  $w(t)$ . Collisional electron viscosity in Ohm's law introduces a cutoff scale length, which, if below the skin depth, does not substantially affect the structures that are found over the scales  $\varrho_s$  and  $d_e$  and the cross-shaped structure (see also Refs. [15,16]). Of course, viscosity spoils the Hamiltonian structure of the model and leads to the reconnection of the fields  $G_{\pm}$ . In the long term, a small dissipation may lead to a steady state reconnection process.

The formation of a new structure for the current density layer in collisionless and semicollisional regimes was already noted in Refs. [12,17]. In the semicollisional regime [17], electron-ion collisions are more important than the electron inertia in providing the effective impedance to the parallel electric field, but  $\varrho_s$  is larger than the reconnection layer width, so this regime can be compared with our results in the limit  $\varrho_s > d_e$ . Our work is the first clear identification of the cross-shaped structure for the current density and vorticity layers and its interpretation in terms of the Casimirs, which are only approximately conserved in the semicollisional regime.

The important difference between Hamiltonian and dissipative reconnection [18] can now be clarified. Both these processes require the localized violation of the topological constraints on the magnetic flux,  $\psi$ . In Hamiltonian plasma models, topological constraints continue to be present, but they involve new fields,  $F$  or  $G_{\pm}$  in the model we have discussed, which differ from  $\psi$  by current density and plasma vorticity terms. Therefore, reconnection of  $\psi$  can proceed unimpeded only by the conservation of  $F$  or of  $G_{\pm}$  if current and vorticity layers are formed.

In the presence of dissipation, the topological constraints relax and the current and vorticity layers are limited by diffusion. On the contrary, in Hamiltonian reconnection the presence of the locally conserved fields makes these layers increasingly sharper and leads to the

formation of microscales. Thus, Hamiltonian reconnection is intrinsically a non-steady-state process. In the time asymptotic limit, these microscales become unphysical and dissipative processes must intervene. However, the correct treatment of the long time evolution is likely to require kinetic considerations. One should note that electrons are accelerated in a narrow layer to very large speeds along the magnetic field lines. Thus, the electron distribution function tends to become highly distorted and one can think of velocity space instabilities (e.g., of the streaming type) which would limit this tendency, introducing an effective (anomalous) current diffusion. Magnetic stochasticity associated with 3D effects is another possibility. Nevertheless, our analysis is valuable in that it suggests possible links between spatial structures and the conservation of the phase-space volume associated with collisionless kinetic models.

It is a pleasure to acknowledge helpful conversations with S. Bulanov, B. Coppi, M. Ottaviani, J. Rem, and T. Schep. This work was supported in part by the ENEA and by the Italian National Research Council (CNR).

- 
- [1] V.M. Vasyliunas, *Rev. Geophys. Space Phys.* **13**, 303 (1975), and references therein.
  - [2] A.W. Edwards *et al.*, *Phys. Rev. Lett.* **57**, 210 (1986).
  - [3] J. Wesson, *Nucl. Fusion* **30**, 2545 (1990).
  - [4] M. Ottaviani and F. Porcelli, *Phys. Rev. Lett.* **71**, 3802 (1993).
  - [5] P.J. Morrison and R.D. Hazeltine, *Phys. Fluids* **27**, 886 (1984).
  - [6] B.N. Kuvshinov *et al.*, *Phys. Lett. A* **191**, 296 (1994); B.N. Kuvshinov *et al.* (to be published).
  - [7] H.R. Strauss, *Phys. Fluids* **19**, 134 (1976).
  - [8] T.J. Schep *et al.*, *Phys. Plasmas* **1**, 2843 (1994).
  - [9] R.D. Hazeltine *et al.*, *Phys. Fluids* **28**, 2466 (1985).
  - [10] F. Pegoraro and T. Schep, *Plasma Phys. Controlled Fusion* **28**, 647 (1986).
  - [11] F. Porcelli, *Phys. Rev. Lett.* **66**, 425 (1991).
  - [12] A.Y. Aydemir, *Phys. Fluids* **4**, 3469 (1992).
  - [13] R.B. White, in *Handbook of Plasma Physics*, edited by A.A. Galeev and R.N. Sudan (North-Holland Publishing Company, Amsterdam, 1983), Vol. 1, p. 611.
  - [14] E. Cafaro *et al.*, in *Theory of Fusion Plasmas, 1996, Proceedings of the Joint Varenna-Lausanne International Workshop* (SIF, Bologna, 1996), p. 453.
  - [15] M. Ottaviani and F. Porcelli, *Phys. Plasmas* **2**, 4104 (1995).
  - [16] D. Biskamp *et al.*, *Phys. Plasmas* **4**, 1002 (1997).
  - [17] R.G. Kleva *et al.*, *Phys. Plasmas* **2**, 23 (1995).
  - [18] P.A. Sweet, in *Electromagnetic Phenomena in Cosmic Physics*, edited by B. Lehnert (Cambridge University Press, Cambridge, England, 1958), p. 123; E.N. Parker, *J. Geophys. Res.* **62**, 509 (1957).